Properties of giant dipole resonances within an extended pairing model with a focus on spectral statistics

A. J. Majarshin, Yan-An Luo, Feng Pan, H. Sabri, M. Rezaei, and Jerry P. Draayer

Phys. Rev. C **104**, 024332 — Published 30 August 2021

DOI: 10.1103/PhysRevC.104.024332

Properties of giant dipole resonances within an extended pairing model with a focus on spectral statistics

A. J. Majarshin[1,2,3,*] Yan-An Luo[1], Feng Pan[2,4], H. Sabri[3], M. Rezaei[3], and Jerry P. Draayer[4]
[1] *School of Physics, Nankai University, Tianjin 300071, P.R. China*
[2] *Department of Physics, Liaoning Normal University, Dalian 116029, P.R. China*
[3] *Department of Physics, University of Tabriz, Tabriz 51664, Iran and*
[4] *Department of Physics and Astronomy, Louisiana State University, Baton Rouge, LA 70803-4001, USA*

In this paper, we report on a study of the spectral features associated with dipole resonances in medium mass nuclei ($E \leq 12$ MeV), as revealed in the framework of the *spd*-interacting boson model. The effect of pairing correlations on the theory follows from solutions obtained through an application of the Bethe Ansatz Equation. In general, calculated spectra around the critical point of the vibrational to γ-soft transitions appears to approach that of a Gaussian Orthogonal Ensemble, while near the rotational and vibrational limits of the theory the spectra show more regular behavior. Specifically, the results reveal that the statistical features of the spectra are sensitive to the vector boson pairing strength, c_p, in the transition region; that is, when c_p is zero, or when the system approaches one of its dynamical symmetries limits the spectrum display regular features, while for stronger c_p values, or when near to the critical phase transition region, the spectral feature show more chaotic behavior. Overall, our results indicate that the statistical features are governed by the interplay between dipole resonant energies, pairing correlations, and interactions between and among the single and vector bosons modes of the theory. As part of this work we also found out that chaoticity occurs when results were fit to a Berry-Robnik distribution. Throughout our analyses, we used experimentally known information about both positive and negative parity states. Our findings suggest that dipole resonances appear to be best-described by Poisson statistics for A $\approx$ 32-138 nuclei.

Keywords: Giant dipole resonance, Pairing correlations, Spectral statistics.

I. INTRODUCTION

High-resolution photo-nuclear experiments have been used for many years to explore special features of nuclear structure. Most recently they have been used to examine spectral statistics of dipole resonances, which in turn has provided a unique opportunity to investigate physical realizations of Gaussian Orthogonal Ensembles (GOE) and Poisson distributions. These special features, as understood within the general framework of Random Matrix Theory (RMT) [1–3], can, in turn, be used to decipher whether a system displays chaotic or regular behavior by comparing nearest-neighbor spacing distribution (NNSD) to Poisson and Wigner [1–5] distributions, respectively. In this paper, building froward on the work of Maino *et* al. [6] on the *spd*-Interacting Boson Approximation (IBA) model, we use an extended version of the theory to study dipole resonances. Properties of giant dipole resonance (GDR) have also been explored by other authors [7–10]. Specifically, resonances of this type have also been examined using Hartree-Fock-Bogoliubov approaches [11], the Random Phase Approximation [12, 13], as well as various other IBA-based theories [6, 14–27].

The IBA, as proposed by Arima and Iachello, includes two types of bosons with angular momentum L=0 (s bosons) and L=2 (d-bosons) [28–30]. Building forward from this, and following the work of Maino *et* al. [6, 17], in this paper we consider the spectral statistics of GDR with an apparent Berry-Robnik Distribution (BRD). Specifically, the scope of the present work is to describe dipole spectra by coupling a p-boson to the IBA *sd*-boson system for a theory with three pairing control parameters (c_s, c_d and c_p), and study the spectral statistics of the resultant high-lying dipole states. A focus on dipole states within such a framework started with the initial work of Morrison and Weise's in 1982 [16] and independently, by Scholtz and Hahne in 1983 [21] Subsequently, Rowe and Iachello in 1983 [8] proposed analytic results by extension of the IBA for energies and transition matrix elements. Maino *et* al. [6, 17, 23, 25, 27] have advanced such investigation from different points of view, such as dipole resonances in the light and odd-even nuclei. Recently, other authors have profferred that the presence of vibrational and low-lying rotational modes coupled to high-lying giant resonances in nuclei could be studied within the (*spd*-IBA)[8, 16, 21, 31].

This integration of the IBA and GDR modes - especially for transitional nuclei - has also been discussed in Refs. [6, 14, 16, 18–27]. An important additional advantage of using a mixed-mode *spd*-IBA system of this type is that it allows one to re-examine resultant level spacings in terms of their regularity and/or chaoticity. Accordingly, in what follows we report on results for ground and excited states of dipole resonance within this framework. In short, we find different degrees of chaoticity with a variation in the pairing strength by performing finite-size scaling up to N=10 bosons.

* jalili@nankai.edu.cn; jalili@tabrizu.ac.ir

Our approach is distinct from others that build directly on the work of Iachello and co-workers ([29, 30, 32–35]). Specifically, we utilize exact solutions of the IBA as advanced by Pan and co-workers [36–42]; and further, we use an affine SU(1,1) algebraic technique to determine the properties of nuclei in the U(5) ⊗ U(3) → SO(9) transitional region of IBA. The latter requires the Hamiltonian be diagonalized numerically, as in Refs. [36, 43–45].

The remainder of this paper is organized as follows: In Sec. II (Theoretical Framework), the dipole mode's coupling to the *sd* boson model is expressed within the SU(1,1) framework. Sec. III (Numerical Results) focuses on comparisons with exact results in *spd*-IBA for different sets of parameters. Also, to describe the NNSD, all level sequences of dipole resonance are prepared from the pairing model and classified based on their pairing strength. Sec. IV (Summary and Conclusion) is a brief recap of essential results. And Sec. V (Acknowledgments) recognizes the various funding sources that enabled this work.

II. THEORETICAL FRAMEWORK

The problem of missing levels hampers most statistical analyses of nuclear data. To address this issue, we analyze dipole states within the framework of an extended *spd*-IBA theory, where a comprehensive analysis of the GDR uses IBA methodologies for same-parity states and a dual pairing mode construction as realized through a SU(1,1) Lie algebra construction for opposite parity configurations. We tested this methodology for a *spdf* boson system [46] by analyzing the affine SU(1,1) Lie algebra within an IBA framework, focusing on low-lying dipole and octupole strengths. The results of that study suggested that some properties of GDR in collective states could be used as indicators of chaos and/or regularity in the mass region of shape phase transitions. If we restrict ourselves to a study of positive parity and low-lying collective states, s and d bosons are sufficient for a complete accounting of spectra excitations (no missing levels) and at the same time, within this framework, the *sd*-IBA can account for collective monopole and quadrupole modes. The present work is focused on the spectral statistics of p bosons and GDR structures.

In recent years, the use of the Richardson model [47, 48] has gained prominence, and extensions to it based on the use of the Bethe Ansatz have been advanced [49, 50]. For these infinite-dimensional algebraic Bethe Ansatz approaches, the pairing Hamiltonian solutions are provided through a set of highly nonlinear Bethe Ansatz Equations (BAE) [51–53]. By exploiting a dual algebraic structure [54, 55] for a multi-level pairing model within an affine SU(1,1) Lie algebra, we can generate exact solutions of the three-level (*spd*-IBA) model for eigenvalues of dipole resonances in the transitional region of medium mass nuclei. And in addition, we can use the *spd*-IBA to determine level spacings and their statistical behavior. So in summary, in this paper we report on results of an application of the algebraic Bethe Ansatz method, within the framework of an infinite-dimensional SU(1,1) Lie algebra [36, 39], to generate the spectrum of the dipole states and use the results to examine the statistical behavior (chaotic and regular) of the dipole states so generated.

A. *spd* Model

To investigate the properties of GDR, similar to that of the two-level system in *sd* boson system, a three-level system in s, p, and d boson model is considered here. In order to analyze the QPT between the spherical and rotational shapes, similar to Refs. [36, 39], the SU(1,1) pairing algebra is produced by $S^{\rho}(l)$, $\rho = 0$, and $\pm$, which satisfies the following commutation relations:

$$[S^{+}_{(l)}, S^{-}_{(l)}] = -2S^{0}_{(l)}, \qquad [S^{0}_{(l)}, S^{\pm}_{(l)}] = \pm S^{\pm}_{(l)}, \tag{1}$$

where l represents s, p and d boson with the angular momentum of 0, 1, and 2, respectively.

The creation operators of SU(1,1) quasi-spin pairing algebras for s, p and d bosons are

$$S^{+}_{s} = (S^{-}_{s})^{\dagger} = \frac{1}{2}s^{\dagger^2}, \quad S^{0}_{s} = \frac{1}{4}(s^{\dagger}.s + s.s^{\dagger}) = \frac{1}{2}n_s + \frac{1}{4}, \tag{2}$$

$$S^{+}_{p} = (S^{-}_{p})^{\dagger} = \frac{1}{2}p^{\dagger}.p, \quad S^{0}_{p} = \frac{1}{4}\sum_{\lambda}(p^{\dagger}_{\lambda}.p_{\lambda}+p_{\lambda}.p^{\dagger}_{\lambda}) = \frac{1}{2}n_p+\frac{3}{4}, \tag{3}$$

$$S^{+}_{d} = (S^{-}_{d})^{\dagger} = \frac{1}{2}d^{\dagger}.d, \quad S^{0}_{d} = \frac{1}{4}\sum_{\lambda}(d^{\dagger}_{\lambda}.d_{\lambda}+d_{\lambda}.d^{\dagger}_{\lambda}) = \frac{1}{2}n_d+\frac{5}{4}, \tag{4}$$

where n_s, n_p, and n_d are the number operators for s, p and d bosons.

The Casimir operator of SU(1,1) for each l boson can be expressed as

$$\hat{C}_2(\mathrm{SU}(1,1)) = S^{0}(l)(S^{0}(l)-1) - S^{+}(l)S^{-}(l). \tag{5}$$

And basis states of an irreducible representation of SU(1,1), $|\kappa\mu\rangle$ for *spd*-IBA, are determined by a single positive real number κ, where $\mu = \kappa, \kappa+1, ...$
Therefore,

$$\hat{C}_2(\mathrm{SU}(1,1))|\kappa\mu\rangle = \kappa(\kappa-1)|\kappa\mu\rangle \qquad S^{0}|\kappa\mu\rangle = \mu|\kappa\mu\rangle. \tag{6}$$

Since the basis vector of U(2l+1) ⊃ O(2l+1) ⊃ O(3) is simultaneously the basis vector of $\mathrm{SU}(1,1)^{l} \supset \mathrm{U}(1)^{l}_{s}$, their complementary relation can be expressed as

$$|N; n\nu LM\rangle = |N, \kappa^{l} = \frac{1}{2}\nu + \frac{1}{4}(2l+1), \mu^{l} = \frac{1}{2}n + \frac{1}{4}(2l+1), LM\rangle, \tag{7}$$

where N, n, ν, L and M is the quantum numbers of U(N),U(2l+1),SO(2l+1),SO(3) and SO(2), respectively. κ^l and μ^l the quantum numbers of U(2l+1) and U(1), respectively. From Eq. (7), it is known that the allowed quantum number n for fixed ν is $n = \nu, \nu+2, \nu+4, ...$, where ν is called the seniority number [56].

The branching rules for the irreps of the algebras of U(n) $\rightarrow$ SO(n), which has been discussed by Hammermesh [57], provide the classification of states for the giant dipole *spd*-IBA model. And pairing models of multi-level configurations are likewise characterized by an overlaid $U(n_1 + n_2 + \cdots)$ algebraic structure[54], which is

$$\begin{aligned} &\mathrm{U_{spd}}(9) \supset \left\{ \begin{array}{c} \mathrm{SO_{spd}}(9) \\ \mathrm{U_d}(5) \otimes \mathrm{U_p}(3) \otimes \mathrm{U_s}(1) \end{array} \right\} \supset \\ &\mathrm{SO_d}(5) \otimes \mathrm{SO_p}(3) \supset \mathrm{SO_d}(3) \otimes \mathrm{SO_p}(3) \supset \mathrm{SO_{pd}}(3). \end{aligned} \quad (8)$$

The operators of infinite dimensional $\mathrm{SU^{spd}}(1,1)$ algebra [36, 39] for GDR are as following.

$$S^{\pm}_m(spd) = c_s^{2m+1} S^{\pm}(s) + c_p^{2m+1} S^{\pm}(p) + c_d^{2m+1} S^{\pm}(d), \quad (9)$$

and

$$S^{0}_m(spd) = c_s^{2m} S^{0}(s) + c_p^{2m} S^{0}(p) + c_d^{2m} S^{0}(d), \quad (10)$$

where c_s, c_p and c_d are the strengths of the different pairings, and m can be taken to be $0, \pm1, \pm2, ...$

The lowest weight states of GDR for $\mathrm{SU^{spd}}(1,1)$ algebra can be defined as

$$\begin{aligned} |lw\rangle^{spd} =& |N^{spd}, \kappa_s = \frac{1}{2}(\nu_s + \frac{1}{2}), \mu_s = \frac{1}{2}(n_s + \frac{1}{2}), \\ & \kappa_p = \frac{1}{2}(\nu_p + \frac{3}{2}), \mu_p = \frac{1}{2}(n_p + \frac{3}{2}), \\ & \kappa_d = \frac{1}{2}(\nu_d + \frac{5}{2}), \mu_d = \frac{1}{2}(n_d + \frac{5}{2}), L, M\rangle, \end{aligned} \quad (11)$$

where $N^{spd} = \nu + \nu_p + \nu_s, n_d = \nu, n_s = \nu_s = 0$ or 1 for *spd*-IBA. Then we have

$$\begin{aligned} S^-(s)|lw\rangle &= 0, \\ S^-(p)|lw\rangle &= 0, \\ S^-(d)|lw\rangle &= 0, \\ S^0_m(spd)|lw\rangle &= \Lambda^{spd}_m |lw\rangle, \end{aligned} \quad (12)$$

where

$$\Lambda^{spd}_m = c_s^{2m}\frac{1}{2}(n_s + \frac{1}{2}) + c_p^{2m}\frac{1}{2}(n_p + \frac{3}{2}) + c_d^{2m}\frac{1}{2}(n_d + \frac{5}{2}). \quad (13)$$

The interaction of the vector boson with the low-energy s and d modes of the GDR can be introduced into the system in the form a duality relation for the *spd* Hamiltonian with a number-conserving unitary part and number-nonconserving quasispin made by using the generators of the $\mathrm{SU^{spd}}(1,1)$ algebra for the transitional region between the two limits. The pairing part of such a model is given as for the *sd*-IBA. Specifically, the Hamiltonian used to explain the spectral structure of the *sd*-IBA can be written as

$$\begin{aligned} &\hat{H} = \varepsilon_s n_s + \varepsilon_p n_p + \varepsilon_d n_d - G \sum_{j=s,d} c_j S^+_j \sum_{j'=s,d} c_{j'} S^-_{j'} + \\ &\beta_p \nu_p(\nu_p + 1) + \beta_d \nu_d(\nu_d + 3) + \gamma_p L_p(L_p + 1) + \\ &\gamma_d L_d(L_d + 1) + \gamma L(L + 1). \end{aligned} \quad (14)$$

Since the energy of the p-boson is higher than those of the s and d bosons, only the two simplest cases with $n_p = 0$ and $n_p = 1$ are considered in this study, from which it follows that p-boson pairs do not need to be considered, and Eq. (14) can accordingly be reduced to the following:

$$\begin{aligned} &\hat{H} = c_s^2 S^0_s + c_d^2 S^0_d - G \sum_{j=s,d} c_j S^+_j \sum_{j'=s,d} c_{j'} S^-_{j'} + \alpha_p \nu_p + \\ &\beta_d \nu_d(\nu_d + 3) + \gamma_d L_d(L_d + 1) + \gamma L(L + 1), \end{aligned} \quad (15)$$

where α_p, β_d, γ_d and γ are real parameters. For simplicity, some of the weak couplings to Casimir operators are not included in this result.

To find the non-zero energy eigenstates with k-pairs, we exploit a Fourier-Laurent expansion of the eigenstates. And the eigenvectors of the Hamiltonian for excitations can be written as

$$\begin{aligned} &|k; \nu_s \nu_d \nu_p n_\Delta L M\rangle = \\ &\sum_{n_i \in Z} a_{n_1 n_2 .... n_k} x_1^{n_1} x_2^{n_2} x_3^{n_3} ... x_k^{n_k} S^+_{n_1} S^+_{n_2} S^+_{n_3} ... S^+_{n_k} |lw\rangle. \end{aligned} \quad (16)$$

By using the commutation relations of Eq. (1), it can be verified that all coefficients $a_{n_1 n_2 .... n_k}$ in Eq. (16) can be taken to be 1, then the wave functions can be expressed simply as

$$\begin{aligned} &|k; \nu_s \nu_d \nu_p n^s_\Delta L_s n^d_\Delta L_d n^p_\Delta L_p M\rangle = \\ &\sum_{n_i \in Z} N' x_1^{n_1} x_2^{n_2} x_3^{n_3} ... x_k^{n_k} S^+_{n_1} S^+_{n_2} S^+_{n_3} ... S^+_{n_k} |lw\rangle, \\ S^+_{x_i} =& \frac{c_s}{1 - c_s^2 x_i} S^+(s) + \frac{c_d}{1 - c_d^2 x_i} S^+(d) + \frac{c_p}{1 - c_p^2 x_i} S^+(p), \end{aligned} \quad (17)$$

where N' is a normalization constant.

In dealing with the seeming complexity of this last expression, a very useful identity known as the BAE [36] can be employed,

$$\frac{\alpha}{x_i} = \sum_{l=0}^{2} \frac{c_l^2(\nu_l + \frac{2l+1}{2})}{1 - c_l^2 x_i} - \sum_{j \neq i} \frac{2}{x_i - x_j}, \quad (18)$$

where ν_s, ν_p, and ν_d are seniority number of s-, p- and d-bosons, respectively. And from this, it follows that the eigenvalues $E^{(k)}$ of Hamiltonian Eq. (15) can be written as

$$E^{(k)} = h^{(k)} + \alpha_p \nu_p + \beta_d \nu_d(\nu_d + 3) + \gamma_d L_d(L_d + 1) + \gamma L(L + 1) + \alpha \Lambda_1^l,$$

$$h^{(k)} = \sum_{i=1}^{k} \frac{\alpha}{x_i}. \tag{19}$$

III. NUMERICAL RESULTS

A. Calculation of dipole resonances

In what follows we report on outcomes of our use of the vector boson concept to create excited dipole states and our analyzes of various aspects of the associated spectra. The pairing model for the $L_p \otimes L_d$ coupling enables these GDR's calculations to be carried out in large configuration spaces. The values of the parameters in the *spd*-IBA Hamiltonian were determined using Least Square Fitting (LSF) methodologies [36]. Numerical results for negative parity states of even-even systems with N=6-10 were determined by solving the associated BAEs.

As shown in [36, 58–66], there are many nuclei in the medium mass region that display spherical to γ-soft phase transition characteristics. Our results for the GDR behavior, calculated for each boson number within the framework the algebraic *sd*-IBA, were studied as a function of the pairing strength. The results were then used to analyzed the dipole resonance properties of the ground and excited state spectra within the *spd* framework. In short, we computed the theoretical dipole spectra for the transitional region via Hamiltonian (15). In Table I we list the set of Eq. (15) solutions, which were extracted by solving the BAE for different k pairing with c_s=[0.1-0.63] and c_p=0. Due to similar correspondences, we do not present BAE calculations for other pairings.

One of the main challenges is to get the position of the dipole states correct, especially answering the question: 'What is the position of the lowest 1^- in our calculation?' One must keep in mind that it should be lower in energy than the coupling $1\otimes 0$, where 0 is the ground state's angular momentum in *sd*-IBA. For excited states of dipole resonance, we have $L_p \otimes L_d$, where L_p and L_d are the angular momentum of the vector and excited state bosons in *sd*-IBA, respectively. In the past we have used the *spd*-IBA model with up to *1p*-boson to describe dipole-excitation states, as $1p$-boson is enough to get the GDR with the coupling of L_d. In this paper, we have selected L_d's coupling from 0 to 12 to get a far better fix on the GDR. It should be mention that to produce 1^+ states, we need at least $2p$-bosons. But here we only focus on GDR, which is related to 1^- states.

As the examples of our present technique suggest, the level spacing of the GDR, determined within the

TABLE I. Solutions of (15) with c_s=[0.1-0.63], c_p=0, α=1100 and G=1.

N	ν_s	ν_d	k	$x_i^\zeta (i = 1, 2, ..., k; \zeta = 1, 2, ..., k + 1)$
6	0	1	2	(1) 99.5016, 99.8388
				(2) 99.7541, 0.996828
				(3) 0.991105, 0.995648
6	1	2	1	(1) 99.3669
				(2) 0.995926
6	0	3	1	(1) 99.5025
				(2) 0.995025
7	1	1	1	(1) 15.9412, 15.9867
				(2) 15.9784, 0.997845
				(3) 0.995648, 0.998348
7	0	2	2	(1) 15.9607, 15.996
				(2) 15.9928, 0.997144
				(3) 0.99777, 0.994746
7	1	3	1	(1) 15.9413
				(2) 0.995023
7	0	4	1	(1) 15.9608
				(2) 0.994124
8	0	1	3	(1) 6.90819, 6.92349, 6.92209
				(2) 6.89071, 6.91405, 0.996826
				(3) 6.89071, 0.995648, 0.998348
				(4) 0.991105, 0.997844, 0.994011
8	1	2	2	(1) 6.89978, 6.91947
				(2) 6.91586, 0.997143
				(3) 0.99291, 0.994745
8	0	3	2	(1) 6.90823, 6.92349
				(2) 6.92209, 0.996426
				(3) 0.991832, 0.991832
8	1	4	1	(1) 6.89983
				(2) 0.994121
8	0	5	1	(1) 6.90827
				(2) 0.993223
9	1	1	3	(1) 4.32433, 4.33668, 4.33442
				(2) 4.3128, 4.32931, 0.996824
				(3) 4.32433, 0.997843, 0.994008
				(4) 0.995646, 0.998347, 0.991102
9	0	2	3	(1) 4.32963, 4.3392, 4.33833
				(2) 4.33329, 4.33953, 0.994745
				(3) 4.33953, 0.989891, 0.99777
				(4) 0.995921, 0.997143, 0.992909
9	1	3	2	(1) 4.32437, 4.33669
				(2) 4.33443, 0.996424
				(3) 0.991827, 0.995017
9	0	4	2	(1) 4.32966, 4.3392
				(2) 4.33833, 0.990765
				(3) 0.995695, 0.994119
9	1	5	1	(1) 4.32441
				(2) 0.993218
10	0	1	4	(1) 2.51335, 2.5189, 2.51839, 2.50699
				(2) 2.51909, 2.51547, 2.5189, 0.99682
				(3) 2.50699, 2.51909, 0.998348, 0.991103
				(4) 2.51335, 0.99682, 0.994005, 0.997842
				(5) 0.991103, 0.998348, 0.995647, 0.99682
10	1	2	3	(1) 2.5103, 2.51745, 2.51614
				(2) 2.50362, 2.51318, 0.995912
				(3) 2.50362, 0.997139, 0.9929
				(4) 0.994741, 0.997768, 0.989884
10	0	3	3	(1) 2.51337, 2.5189, 2.5184
				(2) 0.507031, 2.51548, 0.996422
				(3) 2.5191, 0.991823, 0.995012
				(4) 0.988704, 0.993844, 0.997167
10	1	4	2	(1) 2.51033, 2.51745
				(2) 2.51615, 0.994106
				(3) 0.987532, 0.992942
10	0	5	2	(1) 2.51339, 2.51891
				(2) 2.5184, 0.99321
				(3) 0.986393, 0.992051
10	1	6	1	(1) 2.51036
				(2) 0.992307

spd-IBA framework, is given for different boson numbers. Specifically, we have taken 876 level spacings for 1^- states, and determined eigenenergies of GDR with c_s=[0.1-0.63] with different pairings for all boson numbers from N=[6-10]. For the *sd*-IBA parameters we used those given in Ref. [36], but for *p*-boson parameters, we fit the results to the first experimental $J^p = 1^-$ ground state for each case considered. Specifically we fixed the parameters of the theory using the following input values: $\alpha_p = 885e^{-0.09N}keV$, $\beta_d = 500e^{-0.78N}keV$, $\gamma_d = -8.0e^{-0.07N}keV$ and $\gamma = 23.5e^{-0.16N}keV$.

Throughout what follows, the three-level pairing model underpins our consideration of GDR excitations. However, the nuclei included in the analysis also exhibit changes from vibrational to γ-soft spectral features as N increases. So while the dipole energy spectra are prominent, the analysis also includes a consideration of the associated spectral statistics.

B. Spectral statistics of dipole resonances

To characterize spectral behavior, we use the standard measure of the probability density $P(s)$ of adjacent levels; that is, we use the nearest-neighbor spacing distribution (NNSD, which is the probability of two nearest-neighbor energy levels with the same spin and parity of having a spacing s, see [67]) as captured by $P(s)$ from the unfolded spectrum. Or stated more simply and succinctly, $P(s)$ is a smoothed approximation to the NNSD that is defined as the energy difference ($s_i = \tilde{E}_{i+1} - \tilde{E}_i$) for two adjacent levels of the same spin and parity.

In the unfolding process, we normalized the average level spacing by $d =< s >$, so data with different average level spacing have different chaoticity. As is commonly accepted, the Poisson distribution is defined by

$$P(s) = e^{-s}, \tag{20}$$

which is almost identical to the regular dynamics [68–70]. While the GOE distribution generically represents the NNSD of systems with Wigner dynamics.

$$P(s) = \frac{1}{2}\pi s e^{-\pi s^2/4}. \tag{21}$$

The criteria of chaoticity in energies level distributions is defined in terms of departures from these standard Poisson and Wigner distributions [69–71].

Depending on the details of the chaoticity, some simple distributions have been proposed for describing the spectral statistics of nuclei [72–78] with less fitting parameters. For example, in what follows we use the so-called Berry-Robnik Distribution (BRD), which interpolates between Poisson statistics with q=1 and GOE with q=0, respectively. In the transition from one limit to another limit for the *spd*-IBA, values of the chaoticity range between 0 and 1 with intermediate statistics showing more or less regular behavior as one departs from the two limits. Specifically, In what follows, our use of BRD is defined as advance in [73, 79]

$$P(s,q) = [q + \frac{1}{2}\pi(1-q)s]\exp(-qs - \frac{1}{4}\pi(1-q)s^2), \tag{22}$$

which exhibits Poisson and GOE limits by q=1 and 0. (In studying spectral statistics of energy sequences, a comparison of sets of histograms of sequences with the BRD is made to extract a best overall value for q.)

Another distribution that can used to simplify NNSD data is the so-called cumulative distribution [69, 71, 80]. To further validate and complement our BRD analysis, we have also employed the cumulative distribution, which is defined in terms of the following:

$$I(s) = \int_0^s P(s^{'})ds^{'}. \tag{23}$$

For the Poisson cumulative distribution, we have

$$I_P(s) = 1 - exp(-s). \tag{24}$$

For the corresponding Wigner cumulative distribution, we have

$$I_W(s) = 1 - exp(-\pi s^2/4). \tag{25}$$

Our analysis of the statistical properties of the dipole spectrum includes all states from the ground state up to states at 6 MeV. To ensure convergence within this range, the model spaces for states in the separate *p* space, solved using BAE results, and in the *sd* spaces, solved using *sd*-IBA, had to include all spin and parity states from the BAE results of the *sd*-IBA ranging from N=6 up to N=10. The total angular momentum of specific states is of course determined by the coupling $L_p \otimes L_d$, where L_p and L_d are the angular momenta of the vector and excited state bosons. The first sets of results are shown in Fig. 1, where we group energy spectra of all boson numbers for c_p=0, 0.3, 0.6, and 0.9 pairing strength.

In what follows, we examine spectra results calculated first in the absence (c_p=0) of vector boson pairing, and secondly in the presence of several selected ($c_p \neq 0$) values of the vector boson pairing. Although the detailed results of these calculations are not included in this paper, the fact that the NNSDs of dipole resonances are strongly dependent upon pairing strength is illustrated through the statistical measures noted above and the results that are provided below. This approach allows us to focus on the statistical properties of the spectra of the dipole states calculated based on the BAE and pairing models as systematic explored across the full 0-6 MeV energy range, and which in turn, allows us to achieve a more compact and yet comprehensive understanding of level spacing and spectral features of dipole resonances which is the primary purpose of this paper.

First, we consider the *sd* pairing model, c_s, and c_d, for an even-even system (with different seniority numbers)

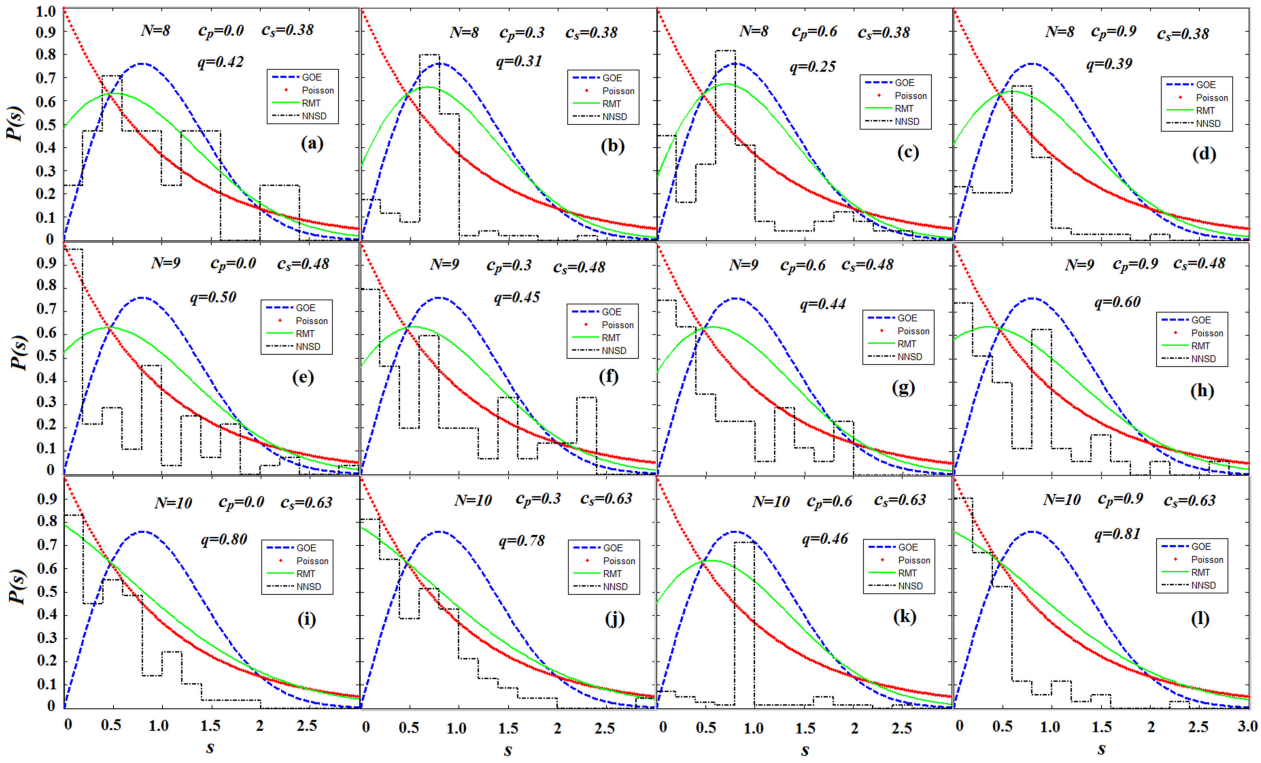

FIG. 1. Spectral statistics of dipole states for different pairing strengths using the RMT and BRD methodologies. Shown are the NNSD of $P(s)$ and histograms obtained from the unfolded energy levels. The green curves show the RMT of BRD interpolating between regular and chaotic patterns. The parameter q was determined by fitting the GDR results for the NNSD for each level sequence of pairing. We compared the different sequences, and each set of GDRs has converted into a set of normalized spacing. Due to the few numbers of levels for N=6 and N = 7 bosons, they are not shown.

up to k=5 pairs. The pairing strength for c_s and c_d are similar to those used in Ref. [36] for *sd*-IBM. In the dipole sector, we calculated theoretical dipole states by varying the vector boson c_p pairing strength. Overall, we chose to consider sequences with 220 spacings for each pairing group, including all levels below 6 MeV. In the *sd*-sector, bosons from N=6 to N=10 were included in the analyses.

The value of the chaoticity measure q, as shown in Fig. 1, was deduced from an analysis of the corresponding NNSD. By increasing the c_p values, we obtained a GOE-like distribution around c_p=0.6; specifically, our results show that level statistics obey a GOE distribution in the QPT (critical) region [81]. Changing the values of c_s and c_p between 0 and 1 causes the system to transition from one dynamical symmetry U(5) to the other SO(9). The pairing strengths also play an essential role in determining the position of the dipole resonance. As illustrated in the Figures, the $P(s)$ without extra pairing (c_p=0) looks like the *sd*-IBM spectrum, but with c_s=0.1 and c_s=0.63, $P(s)$ tends to be of the Poisson type. When the model space is expanded to N=8 and N=9, the nearest-neighbor level spacing distribution looks like a GOE distribution. In a complementary alternative analysis, we also examined the effect of pairing correlations on chaoticity by varying vector boson pairing away from 0.3 to 0.6 with the ratio of c_p/c_s=0.83 and 1.25, the nearest-neighbor level spacing distribution $P(s)$ evolved in the direction that is consistent with GOE statistics. When the pairing interaction is even stronger, at around c_p=0.9, a Poisson-type behavior emerges with the ratio of c_s to c_p being c_p/c_s=1.42.

Spectral statistics have been computed for all energy spectra by increasing the pairing strength. Spectral statistics of the dipole states computed by *spd*-IBA for different pairings are displayed in Figs. 2-5.

The *spd*-IBA calculations provide interesting results. Near those two limits, the system displays a regular pattern. However, by increasing the pairing strength in the transition region, we observe the onset of chaos, which is compatible with the prediction of Alhassid *et al.* [82, 83]. As the number of states for N=6 and N=7 are relatively less, we can extend and work out the level number variance up to N=10. The strongest correlations with three different control parameters for the *spd*-IBA model are found for N=8 and N=9 nuclei. We can conclude that the coupling between the vector and d boson components modifies the spectrum, and the NNSD becomes the intermediate surmise.

The nuclear dipole states are well separated, as those of c_p = 0.0 and c_p = 0.9 in the average level spacing $< d > \approx$ 248.8 and 154.2 keV, respectively. In compari-

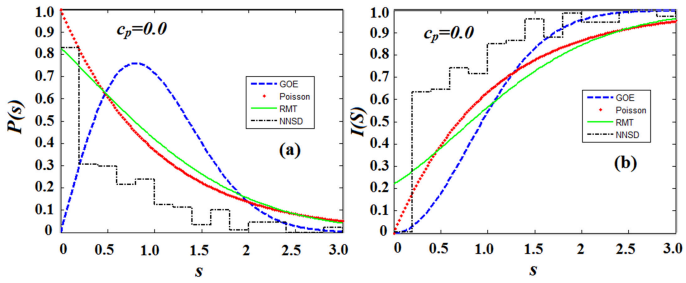

FIG. 2. Spectral statistics of dipole states for different pairing strengths using the RMT and BRD methodologies. Shown are the NNSD of $P(s)$ and integrated NNSD of $I(s)$ and histograms obtained from the unfolded energy levels for c_p=0. The green curves show the RMT of BRD interpolating between regular and chaotic patterns. Fitting the BRD to the data, we obtain q=0.82. With this strength of pairing, we are near to the dynamical symmetry of vibrational limit.

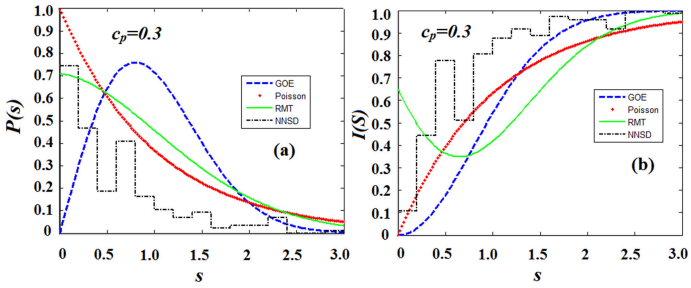

FIG. 3. Spectral statistics of dipole states for different pairing strengths using the RMT and BRD methodologies. Shown are the NNSD of $P(s)$ and integrated NNSD of $I(s)$ and histograms obtained from the unfolded energy levels for c_p=0.3. The green curves show the RMT of BRD interpolating between regular and chaotic patterns. Fitting the BRD to the data, we obtain q=0.70. With this strength of pairing, we are in the transition region of vibrational and γ-soft limit.

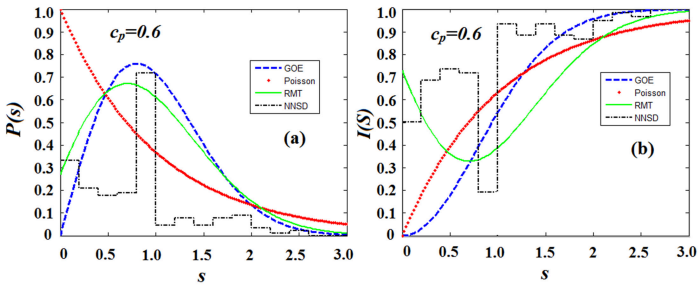

FIG. 4. Spectral statistics of the dipole states computed by *spd*-IBA. Shown are the NNSD of $P(s)$ and integrated NNSD of $I(s)$. Histograms were obtained from the unfolded energy levels for the pairing of c_p=0.6, and the green curves show the RMT of BRD interpolating between regular and chaotic patterns. Fitting the BRD to the data, we obtain values for q=0.26. With this strength of pairing, we are in the transition region of vibrational and γ-soft limit.

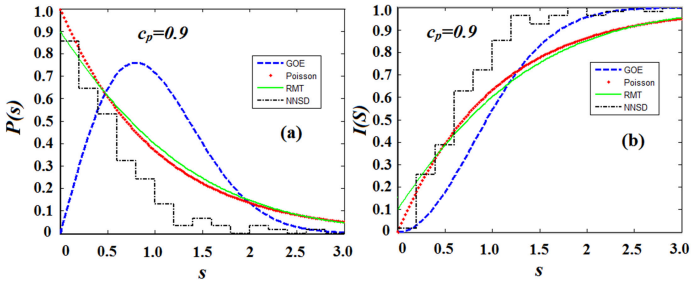

FIG. 5. Spectral statistics of dipole states for different pairing strengths using the RMT and BRD methodologies. Shown are the NNSD of $P(s)$ and integrated NNSD of $I(s)$ and histograms obtained from the unfolded energy levels for c_p=0.9. The green curves show the RMT of BRD interpolating between regular and chaotic patterns. Fitting the BRD to the data, we obtain q=0.88. With this strength of pairing, we are near to the dynamical symmetry of the γ-soft limit.

son with well-separated levels, illustrated by the closely spaced levels for the c_p = 0.3 and c_p = 0.6 pairing, the average level spacings are in $< d >\approx$ 111.7 and 16.7 keV, respectively. We can learn that in transition region for closely spaced levels $< d >\approx$16.7, neighboring states contain information about the chaoticity, and the spectrum for this region is chaotic. These properties and trends are consistent with the nuclear system's chaoticity in closely spaced levels [84] that may cause strongly mixed wave function and modify the nuclear structure of many-body systems [85–87]. These neighboring states with strongly mixed wave functions with the same spin and parity are prevalent in the closely spaced levels.

Now we group neighboring states with the same angular momentum quantum numbers. If we group levels with symmetry representation's angular momentum contents, the neighboring levels of coupling $(L_p \bigotimes L_d)$ belong to different classes. In this condition, we expect the NNSD sequence of level spacings to be similar to the GOE distribution. This distribution reveals some short-range order levels as well as significant gaps. In the neighboring states with the same quantum numbers cases, when we have a coupling group for all set of pairing, one can see the onset of spectral chaos at excitation energy in Fig. 6. These energy spectra belong to all c_p=0, 0.3, 0.6, and 0.9 pairing strengths.

The optimal probability of our distribution result is formulated in terms of a Cramer-Rao Lower Bound (CRLB) minimization problem [88]. One of the first aims of estimation theory is the expansion of bounds on the best feasible operation. Such bounds prepare criteria against which we can correlate the carrying out of any proposed estimator. This criterion is the Cramer-Rao bound, which denotes the smallest possible total variance of chaoticity, i.e., an estimator of q. CRLB is the method for obtaining the accuracy of the estimator parameters. If the estimator is a minimum variance estimator, then its parameter variance achieves the lower bound, that is, the Cramer-Rao bound. Thus, to further decrease

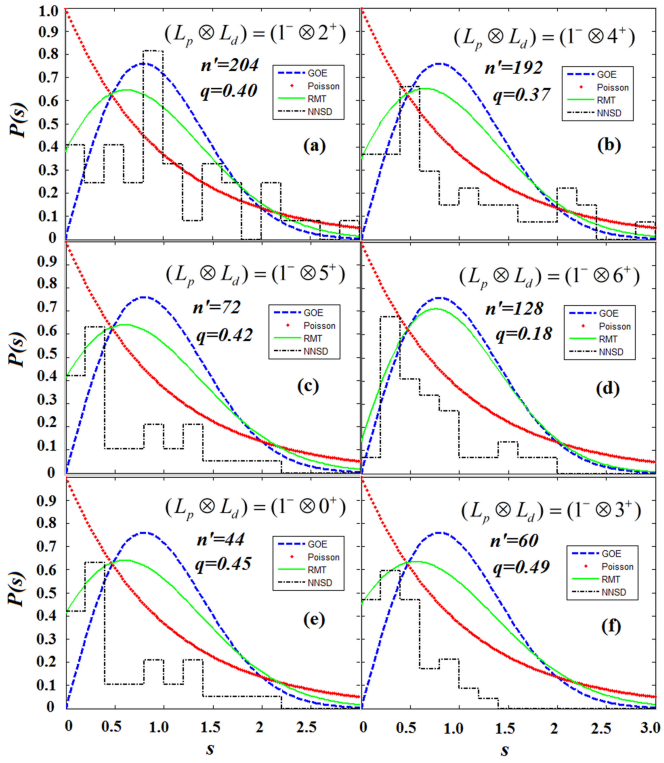

FIG. 6. Spectral statistics of the neighboring levels of coupling $(L_p \bigotimes L_d)$. They are compared to the Poisson (red line) and the GOE (blue line) distribution. Histograms obtained from the unfolded energy levels for all pairing. The corresponding values of the chaoticity parameter q and the number of level spacing n' are given for each coupling. Due to similar correspondences, we do not present the level statistics for those with larger L_d couplings.

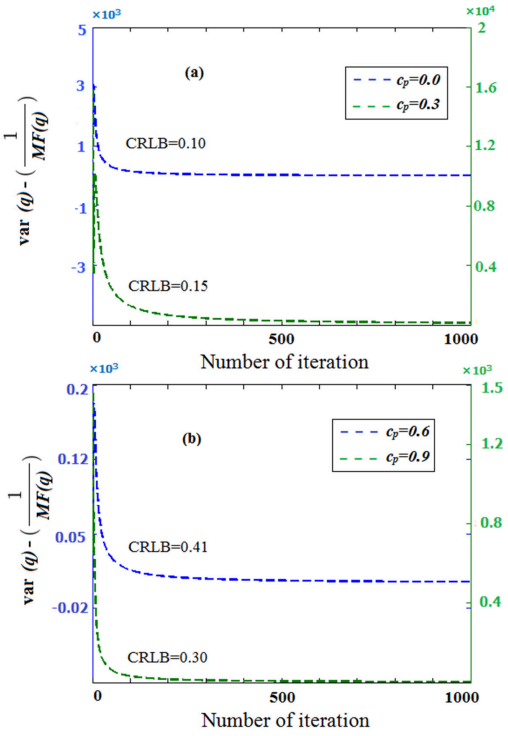

FIG. 7. The variations of CRLBs in the iteration processes for different pairing strength of c_p.

the variance of the minimum variance estimator, one can only optimize the distribution so that the corresponding Cramer-Rao bound is decreased. We have to minimize the errors by CRLB. First, we introduce the Fisher information $F(q)$, and this Fisher information is defined as an optimization problem.

$$F(q) = E\left[\left(\frac{\partial \ln\ P(s;q)}{\partial q}\right)^2\right], \tag{26}$$

where a system in which a quantized version of observation s is used to estimate an underlying parameter q and E denotes the expected value (over s). As the estimation of CRLB is the inverse of the $F(q)$, the variance of the estimator is defined as follows:

$$\mathrm{var}(q) \geq \frac{1}{MF(q)}, \tag{27}$$

where M is the sample size. By calculating $F(q)$, the scalar quantity $\frac{1}{MF(q)}$ is the CRLB on the variances of unbiased estimators. The minimum CRLB corresponds to the final value in the iteration procedure. The Newton-Raphson procedure can be used to approximate the solution q, giving an approximation to the CRLB. This algorithm converges to the exact solution q in τ iterations. The variance estimates of the estimators are obtained by repeating the Newton-Raphson procedure for τ=1000 to get the minimum variance for CRLB. The process is repeated until a sufficiently precise value is reached. However, when carried to termination, it is not computationally competitive with the least square fitting. We have used the least square fitting results as an initial guess for a root of distribution in iterative root-finding procedures.

Finally, to find the efficiencies of considered distribution via fitting, we determined the CRLB, right-hand side of Cramer-Rao inequality (27), as CRLB $\equiv \frac{1}{MF(q)}$. For the final value, q is obtained from fitting processes. We have evaluated the NNSD for different pairing. To compare the efficiencies of BRD in different sequences of dipole resonance by the iteration processes, we have calculated CRLB for different pairing strength of c_p where c_s=0.1 and c_p=0 has the least CRLB by comparison with other pairing strength. The variations of CRLBs in the iteration processes for different pairing strength of c_p are displayed in Fig. 7.

To get further insight into the nature of GDR's in the medium mass region, we also inspected the sequences of NNSD for the 342 states with $J^p = 1^-$ and for the 97 states with $J^p = 1^+$. In addition to the references cited herein for the pygmy and giant dipole resonances, several workers investigated experimental features in somewhat

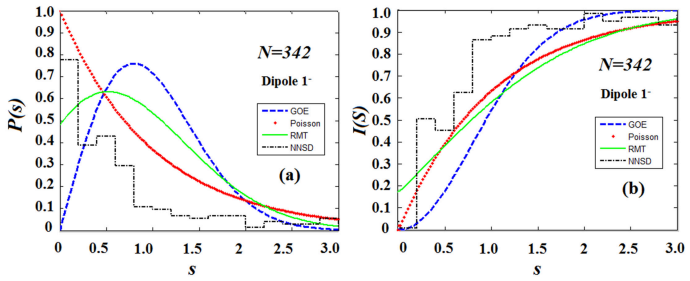

FIG. 8. Spectral statistics of the experimental dipole states $J^p = 1^-$. Shown are the NNSD of $P(s)$ and integrated NNSD of $I(s)$. Histograms obtained from the unfolded energy levels for the $J^p = 1^-$ states. Fitting the BRD to the data, we obtain q=0.81.

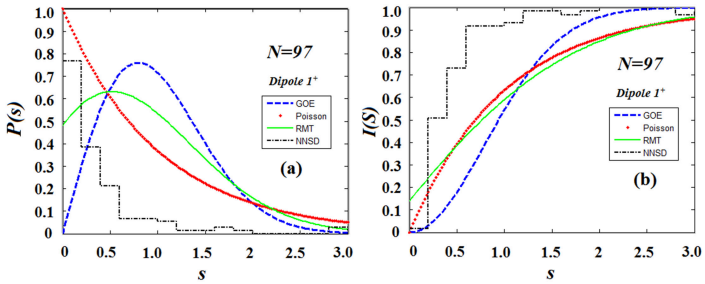

FIG. 9. Spectral statistics of the experimental dipole states $J^p = 1^+$. Shown are the NNSD of $P(s)$ and integrated NNSD of $I(s)$. Histograms obtained from the unfolded energy levels for the $J^p = 1^+$ states. Fitting the BRD to the data, we obtain q=0.87.

light and medium nuclei. These include from ^{32}S to ^{138}Ba [89–102]. The lowest and highest experimental dipole states with the number of selected levels are listed in Tables II and III.

The calculated chaoticity values together with NNSD displayed in Figs. 8 and 9 reveal some regularity in dipole resonances. We analyzed the NNSD for the positive $J^p = 1^+$ and negative $J^p = 1^-$ parity states to clarify the chaotic and regular spectral properties on validated GDR. For these modes, we find a tendency towards Poisson behavior. Our *spd*-IBA and spectral statistics calculations facilitate a satisfactory description of the GDR's properties in the proposed nuclei. All ground and excited states are included in the calculation of NNSD. Again, variations of CRLBs are shown in Fig. 10 for experimental $J^p = 1^-$ and $J^p = 1^+$ states. In the variations of CRLBs curves, the meaning of the scales on the vertical axis is that it allows the assessment of how close a given estimation method is to optimality. In particular, if the variance of an unbiased estimate is equal to the Cramer-Rao bound, then it has minimum variance. The estimated parameters display a reduction of uncertainties and yield estimator's variances very close to CRLBs, as shown in Figs. 7 and 10. It means that the difference between the left and right sides of Eq. (27) can be used

TABLE II. A description of the available data of dipole negative parity state in the analysis where M describes the number of selected levels and E_i and E_f represents the lowest and the highest level contributed to each nucleus.

Nuclei	M	$E_i(keV)$	$E_f(keV)$	Reference
^{32}S	5	7480	11710	[89]
^{40}Ca	5	6612.2	9545.7	[90]
^{52}Cr	20	5098.6	9236.6	[91]
^{56}Fe	9	6925.4	9287.6	[92]
^{58}Ni	11	7048.2	9723.0	[92]
^{60}Ni	48	6180.6	9892.6	[93]
^{70}Ge	11	4356.6	7753.0	[94]
^{72}Ge	7	5849.5	8441.2	[94]
^{74}Ge	11	4224.9	7652.1	[94]
^{76}Ge	12	5698.9	9013.2	[94]
^{76}Se	76	4601.6	7093.1	[95]
^{86}Kr	23	4867.4	9085.6	[96]
^{88}Sr	48	4742.7	10644.1	[97]
^{90}Zr	15	6295.8	10042.9	[98]
^{116}Sn	32	4547.1	8361.3	[99]
^{124}Sn	35	5842.5	8376.2	[99]
^{138}Ba	9	4025.2	6102.7	[100]

TABLE III. A description of the available data of dipole positive parity state in the analysis where M describes the number of selected levels and E_i and E_f represents the lowest and the highest level contributed to each nucleus.

Nuclei	M	$E_i(keV)$	$E_f(keV)$	Reference
^{50}Cr	15	3628.2	9719.1	[101]
^{52}Cr	25	5098.6	9429.0	[91]
^{56}Fe	7	3448.6	8908.9	[92]
^{58}Ni	8	5905.3	9156.9	[92]
^{60}Ni	32	3193.6	9830	[93]
^{74}Ge	6	3093.4 5	6733.4	[102]
^{76}Se	11	4055.2	7110.1	[95]

to describe the variation (decreasing) of uncertainties for estimated parameters during the iterations. From these curves, it is obvious that the CRLB serves as a good approximation to the estimator's variance, particularly for spherical symmetry with c_p=0.

We have seen from the estimated values of the BRD parameter q shown in Figs. 8 and 9 that level energies near dynamical U(5) and SO(9) symmetries in the *spd*-IBA model seem more regular. Similar to the predictions made by J. Enders in [103], the spectra of medium mass nuclei for dipole states seem almost regular, while for the predictions in light nuclei made by B. Dietz in [72], the spectra for negative and positive parity states are almost regular and chaotic, respectively. It is verified that the NNSD is governed by the interplay between the GDR and the pairing interaction for BAE calculated from the *spd*-IBA model. From theory, based on the spectral

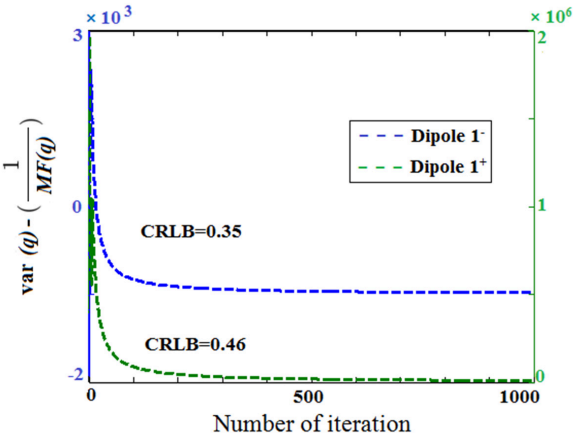

FIG. 10. The variations of CRLBs in the iteration processes for dipole $J^p = 1^-$ and $J^p = 1^+$ states.

statistics for most spectra in *spd*-IBA around dynamical symmetries, vibrational and γ-soft, the NNSDs for dipole states show similar behavior as experiment.

Finally, we conclude that a phenomenological collective model for IBA is the best tool to investigate the spectra for dipole states. This collective model estimates dipole resonances to calculate the level spacing distribution with the pairing model. In addition to its consistency, our *spd*-IBA model in GDR is computationally so simple that it can be easily applied to large sets of collective models, as *sdg* and *sdf*-IBA.

IV. SUMMARY AND CONCLUSION

We conclude that the *spd*-IBA can reproduce dipole states in a wide variety of nuclei. The proposed model and properties of the GDR are investigated in medium mass nuclei ($E \leq 12$ MeV). It has been demonstrated that the *spd*-IBA is a quite powerful tool to investigate nuclear structures. In this paper, We have studied the GDRs within an extended pairing model with a focus on spectral statistics. The next case is the energy spectra that have been analyzed using both the *spd*-IBA and BAE. The effect of pairing correlations on spectral statistics is the primary result of this paper. We have found that varying the pairing interaction strength for vector boson c_p is likely to alter the statistical properties of the spectra. The *spd*-IBA undergoes vibrational to the γ-unstable shape phase transition. We have seen that the dipole spectrum obeyed GOE statistics for boson numbers, which was near the critical point. In contrast, the spectra become regular for those nuclei near either vibrational or γ-unstable points. Because of the appropriate success of the *spd*-IBA in chaos and regularity of nuclei, the investigation of another extension of the IBA in *sdf*, *sdg*, and *spdf* boson systems should be feasible.

V. ACKNOWLEDGEMENTS

Support from the Natural Science Foundation of China (11875171, 11875158, 11675071), Natural Science Foundation of Tianjin (20JCYBJC01510), the US National Science Foundation (OCI-0904874 and ACI-1516338), US Department of Energy (DE-SC0005248); Iran National Science Foundation (INSF: No. 95014287) and the LSU-LNNU joint research program (9961) is acknowledged.

[1] J. M. G. Gómez, K. Kar, V. K. B. Kota, R. A. Molina, A. Relaño, and J. Retamosa, Physics Reports 499, 103 (2011).
[2] A. Severyukhin, S. Åberg, N. Arsenyev, and R. Nazmitdinov, Physical Review C 98, 044319 (2018).
[3] A. Magner, A. Levon, and S. Radionov, The European Physical Journal A 54, 214 (2018).
[4] H. Weidenmüller and G. Mitchell, Reviews of Modern Physics 81, 539 (2009).
[5] V. Zelevinsky, B. A. Brown, N. Frazier, and M. Horoi, Physics reports 276, 85 (1996).
[6] Maino, G., et al. Physical Review C 30.6: 2101 (1984).
[7] D. Kusnezov and W. E. Ormand, Physical review letters 90, 042501 (2003).
[8] Rowe, D. J., and F. Iachello. Physics Letters B 130.5: 231-234 (1983).
[9] Emling, Hans. Progress in Particle and Nuclear Physics 33: 729-785 (1994).
[10] Chomaz, Ph, and N. Frascaria. Physics Reports 252.5: 275-405 (1995).
[11] P. Ring and P. Schuck, The nuclear many-body problem (Springer, Heidelberg,1980).
[12] Roca-Maza, X., et al. Physical Review C 85.2: 024601 (2012).
[13] Hergert, H., P. Papakonstantinou, and R. Roth. Physical Review C 83.6: 064317 (2011).
[14] Scholtz, F. G. Physics Letters B 151.2: 87-89 (1985).
[15] Scholtz, F. G., and F. J. W. Hahne. Physical Review C 34.2: 693 (1986).
[16] Morrison, I., and J. Weise. Journal of Physics G: Nuclear Physics 8.5: 687 (1982).
[17] Maino, G., A. Ventura, and L. Zuffi. Physical Review C 37.4: 1379 (1988).
[18] Andres, M. V., et al. Physics Letters B 470.1: 6-12 (1999).
[19] Alonso, C. E., et al. Nuclear Physics A 679.3: 359-372 (2001).

[20] Hoblit, S. D., and A. M. Nathan. Physical Review C 44.6: 2372 (1991).
[21] Scholtz, F. G., and F. J. W. Hahne. Physics Letters B 123.3-4: 147-150 (1983).
[22] Iachello, F. Physics Letters B 160.1: 1-4 (1985).
[23] Maino, G., et al. Physical Review C 33.3: 1089 (1986).
[24] Scholtz, F. G., and F. J. W. Hahne. Nuclear Physics A 471.3-4: 545-564 (1987).
[25] Maino, Giuseppe. Physical Review C 40.2: 988 (1989).
[26] Turrini, S., G. Maino, and A. Ventura. Physical Review C 39.3: 824 (1989).
[27] Maino, G., A. Ventura, and L. Zuffi. Physical Review C 46.5: 1725 (1992).
[28] Arima, A., and F. Iachello. Physical Review Letters 35.16: 1069 (1975).
[29] Arima, A., and F. Iachello. Annals of Physics 99.2: 253-317 (1976).
[30] Arima, A., and F. Iachello. Annals of Physics 111.1: 201-238 (1978).
[31] A. J. Majarshin, and H. Sabri. Nuclear Physics A 964: 69-85 (2017).
[32] Iachello, Francesco, and Akito Arima. The interacting boson model. Cambridge University Press, (1987).
[33] Scholten, O., F. Iachello, and A. Arima. Annals of Physics 115.2: 325-366 (1978).
[34] Arima, A., and F. Iachello. Annals of Physics 123.2: 468-492 (1979).
[35] Iachello, F. Physical Review Letters 85.17: 3580 (2000).
[36] Pan, Feng and J. Draayer, Nuclear Physics A 636: 156 (1998).
[37] Pan, Feng, and J. P. Draayer. Physics Letters B 442.1: 7-13 (1998).
[38] Pan, Feng, and J. P. Draayer. Annals of Physics 275.2: 224-237 (1999).
[39] F. Pan, X. Zhang, and J. Draayer, Journal of Physics A: Mathematical and General 35, 7173 (2002).
[40] Pan, Feng, V. G. Gueorguiev, and J. P. Draayer. Physical review letters 92.11: 112503 (2004).
[41] Pan, Feng, et al. Physics Letters A 341.1: 291-296 (2005).
[42] Pan, Feng, et al. Physical Review C 91.3: 034305 (2015).
[43] M. A. Jafarizadeh, et al. International Journal of Modern Physics E 1650089 (2016).
[44] A. J. Majarshin and M. A. Jafarizadeh, Nuclear Physics A 968, 287-325 (2017).
[45] A. J. Majarshin, M. A. Jafarizadeh, and H. Sabri. The European Physical Journal Plus 132.10, 418 (2017).
[46] M. A. Jafarizadeh, et al. Journal of Physics G: Nuclear and Particle Physics 43.9, 095108 (2016).
[47] R.W. Richardson, Phys. Lett. 3, 277 (1963).
[48] R.W. Richardson and N. Sherman, Nucl. Phys. 52, 221(1964).
[49] Feng Pan, J. P. Draayer, and W. E. Ormand, Phys. Lett. B 422, 1 (1998).
[50] J. Dukelsky, C. Esebbag, and P. Schuck, Phys. Rev. Lett. 87, 066403 (2001).
[51] A. J. Majarshin, Eur. Phys. J. A 54, 11 (2018).
[52] A. J. Majarshin, H. Sabri, and M. A. Jafarizadeh. Eur. Phys. J. A 54.3: 1-14 (2018).
[53] A. J. Majarshin, et al. Chinese Physics C 45: 2 (2021).
[54] M. Caprio, P. Cejnar, and F. Iachello, Annals of Physics 323, 1106 (2008).
[55] D. Rowe, M. Carvalho, and J. Repka, Reviews of Modern Physics 84, 711 (2012).
[56] F. Iachello and A. Arima, The interacting boson model (Cambridge University Press, 1987).
[57] M. Hamermesh, Group theory and its application to physical problems (Courier Corporation, 1962).
[58] Frank, A., C. E. Alonso, and J. M. Arias. Physical Review C 65.1: 014301 (2001).
[59] Clark, R. M., et al. Physical Review C 69.6: 064322 (2004).
[60] Van Isacker, P., and G. Puddu. Nuclear Physics A 348.1: 125-139 (1980).
[61] Buyokata, M., P. Van Isacker, and I. Uluer. Journal of Physics G: Nuclear and Particle Physics 37.10: 105102 (2010).
[62] Meng, Xiang-fei, et al. Physical Review C 77.4: 047304 (2008).
[63] Zamfir, N. V., et al. Physical Review C 65.4: 044325 (2002).
[64] Kern, J., et al. Nuclear Physics A 593.1: 21-47 (1995).
[65] Hicks, S. F., et al. Physical Review C 86.5: 054308 (2012).
[66] Nomura, K., R. RodrÃguez-GuzmÃ¡n, and L. M. Robledo. Physical Review C 94.4: 044314 (2016).
[67] A. J. Majarshin, et al. Physica Scripta 95.10: 105305 (2020).
[68] H. A. Weidenmüller and G. E. Mitchell, Rev. Mod. Phys. 81, 539 (2009).
[69] A. Levon, A. Magner, and S. Radionov, Phys. Rev. C 97, 044305 (2018).
[70] A. Y. Abul-Magd, H. L. Harney, M. H. Simbel, and H. A. Weidenmüller, Phys. Lett. B 579, 278 (2004).
[71] B. Dietz, A. Heusler, K. Maier, A. Richter, and B. Brown, Phys. Rev. Lett. 118, 012501 (2017).
[72] B. Dietz, B. A. Brown, U. Gayer, N. Pietralla, V. Y. Ponomarev, A. Richter, P. C. Ries, and V. Werner, Physical Review C 98, 054314 (2018).
[73] A. J. Majarshin, F. Pan, H. Sabri, and J. P. Draayer, Annals of Physics 407, 250 (2019).
[74] M. V. Berry and M. Robnik, Journal of Physics A: Mathematical and General 17, 2413 (1984).
[75] M. C. Gutzwiller, Chaos in classical and quantum mechanics (Springer Science Business Media, 2013).
[76] M. Bae, T. Otsuka, T. Mizusaki, and N. Fukunishi, Physical review letters 69, 2349 (1992).
[77] K. Roy, B. Chakrabarti, N. Chavda, V. Kota, M. Lekala, and G. Rampho, EPL (Europhysics Letters) 118, 46003 (2017).
[78] P. Fanto, Y. Alhassid, and H. Weidenmüller, Physical Review C 101, 014607 (2020).
[79] C. Fang-Qi, S. Yang, and Z. Xian-Rong, Chinese Physics C 33, 24 (2009).
[80] L. Muñoz, R. A. Molina, J. Gómez, and A. Heusler, Physical Review C 95, 014317 (2017).
[81] H. Wu and M. Vallières, Journal of Physics G: Nuclear and Particle Physics 16, L149 (1990).
[82] Y. Alhassid., A. Novoselsky, and N. Whelan. Phys. Rev. Lett 65, 24, 2971 (1990).
[83] Y. Alhassid and A. Novoselsky, Physical Review C 45, 1677 (1992).
[84] J. D. Garrett, J. Q. Robinson, A. J. Foglia, and H. Q. Jin, Physics Letters B 392, 24 (1997).
[85] L. Dai, F. Pan, Z. Feng, Y. Zhang, S. Cui, and J. Draayer, Chinese Physics C 44, 064102 (2020).

[86] A. J. Majarshin, Y.-A. Luo, F. Pan, H. T. Fortune, and J. P. Draayer, Physical Review C 103, 024317 (2021).
[87] A. J. Majarshin, Y.-A. Luo, F. Pan, and H. T. Fortune, Physical Review C 104, 014321 (2021).
[88] S. K. Rao, in Conference Record of Thirty-Second Asilomar Conference on Signals, Systems and Computers (Cat. No. 98CH36284) (IEEE, 1998), p. 441.
[89] M. Itoh et al., Physical Review C 88, 064313 (2013).
[90] T. Hartmann, J. Enders, P. Mohr, K. Vogt, S. Volz, and A. Zilges, Physical Review C 65, 034301 (2002).
[91] H. Pai et al., Physical Review C 88, 054316 (2013).
[92] F. Bauwens et al., Physical Review C 62, 024302 (2000).
[93] M. Scheck et al., Physical Review C 88, 044304 (2013).
[94] A. Jung et al., Nuclear Physics A 584, 103 (1995).
[95] P. Goddard et al., Physical Review C 88, 064308 (2013).
[96] R. Schwengner et al., Physical Review C 87, 024306 (2013).
[97] R. Schwengner et al., Physical Review C 76, 034321 (2007).
[98] R. Schwengner et al., Physical Review C 78, 064314 (2008).
[99] K. Govaert, F. Bauwens, J. Bryssinck, D. De Frenne, E. Jacobs, W. Mondelaers, L. Govor, and V. Y. Ponomarev, Physical Review C 57, 2229 (1998).
[100] R.-D. Herzberg et al., Physical Review C 60, 051307 (1999).
[101] H. Pai et al., Physical Review C 93, 014318 (2016).
[102] R. Massarczyk et al., Physical Review C 92, 044309 (2015).
[103] J. Enders, T. Guhr, A. Heine, P. von Neumann-Cosel, V. Y. Ponomarev, A. Richter, and J. Wambach, Nuclear Physics A 741, 3 (2004).